

1 **Title**

2 **A secreted peptide and its receptors shaping the auxin response pattern and leaf**
3 **margin morphogenesis**

4

5 Authors/Affiliations

6 Toshiaki Tameshige^a, Satoshi Okamoto^b, Jin Suk Lee^c, Mitsuhiro Aida^b, Masao Tasaka^b,
7 Keiko U. Torii^{a,c,d,e,1} and Naoyuki Uchida^{a,e,1}

8

9 ^a Institute of Transformative Bio-Molecules (WPI-ITbM), Nagoya University, Furo-cho,
10 Chikusa-ku, Nagoya, 464-8601, Japan

11 ^b Graduate School of Biological Sciences, Nara Institute of Science and Technology,
12 8916-5 Takayama, Ikoma, 630-0192, Japan

13 ^c Department of Biology, University of Washington, Seattle, WA98195, USA

14 ^d Howard Hughes Medical Institute, University of Washington, Seattle, WA98195, USA

15 ^e Division of Biological Science, Graduate School of Science, Nagoya University,
16 Furo-cho, Chikusa-ku, Nagoya, 464-8602, Japan

17

18 Contact

19 ¹ Correspondence: Keiko U. Torii (ktorii@u.washington.edu) and Naoyuki Uchida
20 (uchinao@itbm.nagoya-u.ac.jp)

21 **Summary**

22 Secreted peptides mediate intercellular communication [1, 2]. Several secreted peptides
23 in the EPIDERMAL PATTERNING FACTOR-LIKE (EPFL) family regulate
24 morphogenesis of tissues, such as stomata and inflorescences in plants [3-15]. The
25 biological functions of other EPFL family members remain unknown. Here, we show that
26 the *EPFL2* gene is required for growth of leaf teeth. EPFL2 peptide physically interacts
27 with ERECTA (ER) family receptor-kinases and, accordingly, the attenuation of the
28 ER-family activities leads to formation of toothless leaves. During the tooth growth
29 process, responses to the phytohormone auxin are maintained at tips of the teeth to
30 promote their growth [16-19]. In the growing tooth tip of *epfl2* and multiple *er*-family
31 mutants, the auxin response becomes broader. Conversely, overexpression of *EPFL2*
32 diminishes the auxin response, indicating that the EPFL2 signal restricts the auxin
33 response to the tooth tip. Interestingly, the tip-specific auxin response in turn organizes
34 characteristic expression patterns of *ER* family and *EPFL2* by enhancing the *ER*-family
35 expression at the tip while eliminating the *EPFL2* expression from the tip. Our findings
36 identify the novel ligand-receptor pairs promoting the tooth growth, and further reveal a
37 feedback circuit between the peptide-receptor system and auxin response as a mechanism
38 for maintaining proper auxin maxima during leaf margin morphogenesis.

39 **Results and Discussion**

40

41 ***EPFL2* is required for leaf tooth growth**

42 EPIDERMAL PATTERNING FACTOR-LIKE (EPFL) family peptides
43 represent a group of secreted cysteine-rich peptides [3], which are genetically encoded in
44 diverse land plants including *Arabidopsis thaliana* [20]. Among the eleven *Arabidopsis*
45 EPFLs, EPFL1, 2 and EPFL9/STOMAGEN control stomatal patterning [4-11], while
46 EPFL4, 5 and 6 (also known as CHALLAH [CHAL], CHAL-LIKE1 [CLL1], and CLL2)
47 regulate inflorescence development (Figure 1A) [13-15]. However, the biological roles
48 for other EPFLs including EPFL1, 2 and 3, which constitute a subclade, remain unknown
49 (Figure 1A) [20]. To reveal a role for *EPFL2* gene, we analyzed a mutant line that carries
50 a transposon insertion in the *EPFL2* locus (Figure S1A). The full-length *EPFL2*
51 transcripts were not detected in the mutant (Figure S1A), indicating that the mutant is
52 transcriptionally null for *EPFL2*. This mutant was originally isolated in Landsberg *erecta*
53 (*L.er*) accession that carries a loss-of-function mutation in the *ERECTA* (*ER*) gene [21].
54 Because *ER* is known as the receptor for some EPFL family peptides, the *epfl2*
55 phenotypes were first analyzed in the *L.er* background that harbors the functional *ER*
56 transgene to exclude a possibility that *epfl2* phenotypes might be modified by the *er*
57 mutation. While *epfl2* did not exhibit obvious growth defects, the mutant leaves showed
58 smooth margin in contrast to wild type leaves, suggesting that *EPFL2* plays a role in leaf
59 serration (Figure S1B and S1C). The phenotype was rescued by the introduction of the
60 wild-type *EPFL2* genomic fragment (Figure S1D). The *epfl2* leaves still exhibited the
61 toothless phenotype after introgression into the Columbia (*Col*) accession by outcrossing

62 seven times (Figure 1B and 1D). These data indicate that *EPFL2* is required for leaf tooth
63 development.

64 Serration, or saw-like projections of leaf teeth, are initiated as small primordia
65 along the leaf margin during early leaf development (Figure 1C), and eventually grow to
66 dentate structures in mature leaves (Figure 1B). Tooth primordia are initiated normally in
67 young *epfl2* leaves (Figure 1E), indicating that *EPFL2* is required for tooth growth after
68 the initiation. Tooth growth can be promoted either by outgrowth of the tooth primordia
69 or by growth repression of the sinus tissues between the primordia [22]. To test these
70 possibilities, the outlines from the wild type and *epfl2* leaves at a young stage with a size
71 around 2.5 mm² were superimposed and compared (Figure 1F). If the tooth outgrowth
72 was reduced in the mutant, positions of mutant tooth tips would be located inward from
73 those of wild type without changes in sinus positions [18]. Conversely, if the growth
74 suppression of sinuses was derepressed in the mutant, tip positions would be well aligned
75 between wild type and the mutant, while positions of mutant sinuses would be shifted
76 outward from those of wild type. The superimposed image between wild type and *epfl2*
77 showed that *epfl2* is classified into the former case. Although the sinus positions are well
78 aligned, the tip positions of *epfl2* were located inward from those of wild type (Figure
79 1F). These results support the hypothesis that *EPFL2* contributes to outgrowth of tooth
80 primordia rather than growth repression of sinus tissues.

81 Next, we analyzed the expression pattern of *EPFL2* using *EPFL2pro::GUS*
82 reporter. The GUS signals were broadly detected in growing leaves and, notably, the
83 signals were excluded from tooth tips and developing veins (Figure 1G). This suggests

84 that the *EPFL2* promotes tooth growth from the peripheral region of the tooth, not at the
85 tooth tip.

86

87 ***ERECTA* family genes are required for leaf tooth growth**

88 All the EPFLs characterized to date exert their activities through the ER receptor
89 kinase family consisting of ER, ER-LIKE1 (ERL1) and ERL2 [4-6, 10-15]. To address
90 whether ER-family receptors act in leaf tooth development, we first examined the leaf
91 shape of *er*-family mutants. Each of *er*, *erl1* and *erl2* single mutants developed leaf teeth
92 like the wild type (Figure S1E-S1H). Since ER family is known to act in a redundant
93 manner [23], we next examined each combination of *er*-family double mutants. *er erl1*,
94 *er erl2* and *erl1 erl2* all showed the toothless phenotype resembling that of *epfl2* (Figure
95 1H, 1J and 1L). When young leaves were observed, all of the mutants displayed tooth
96 primordia (Figure 1I, 1K and 1M), indicating that the tooth initiation still occurs in these
97 mutants.

98 Next, we analyzed the shape of growing leaves of the *er*-family double mutants.
99 For this purpose, we focused on *erl1 erl2* rather than *er erl1* and *er erl2*. This is because
100 the *er* mutation affects leaf proportion, such as a ratio of width to length [21, 24], causing
101 misalignments of both tip and sinus positions in superimposed images between wild-type
102 vs. *er erl1* or *er erl2* leaves (Figure S1I). The outlines of growing *erl1 erl2* leaves showed
103 sinus positions well-aligned with those of wild type, while tooth tip positions were
104 located inward from those of wild type (Figure 1N). These results suggest that, like
105 *EPFL2*, *ER* family contributes to outgrowth of tooth primordia rather than growth
106 repression of sinus tissues.

107 We further characterized the expression patterns of *ER*-family genes in growing
108 leaves using *promoter::GUS* reporters [23]. *ERpro::GUS* was expressed broadly
109 throughout young leaves (Figure 1O). *ERL1pro::GUS* signals were also broadly detected,
110 with tooth tips particularly showing strong signals (Figure 1P). Notably, *ERL2pro::GUS*
111 expression was restricted to the tooth tips and some vein precursors (Figure 1Q),
112 contrasting to that of *EPFL2pro::GUS* (Figure 1G). Based on these findings, we conclude
113 that *ER*-family genes redundantly promote leaf tooth morphogenesis at the tooth tips after
114 tooth initiation.

115 The complete absence of three *ER*-family genes conferred severe leaf shape
116 defects, perhaps owing to known defects in the shoot apical meristem and stomatal
117 differentiation [23, 25-27]. Since this made the comparative analysis of leaf margin shape
118 difficult, we focused on the *ER*-family double mutants for further analyses. However, we
119 found that tooth primordia were lost in *er erl1 erl2* triple mutants (Figure S1J and S1K),
120 indicating that *ER*-family may also be involved in the tooth initiation process.

121

122 **EPFL2 peptide and ER-family receptors act as ligand-receptor pairs**

123 Genetic interactions between *EPFL2* and *ER* family were subsequently analyzed.
124 *er erl1 epfl2*, *er erl2 epfl2* and *erl1 erl2 epfl2* triple mutants all exhibited the same
125 toothless phenotype as the parental *epfl2* single and *er-family* double mutants (Figure
126 S2A-S2H). To quantify tooth growth phenotypes between wild-type and *epfl2*, we first
127 applied seven different quantification methods: Height vs. Width Ratio of tooth [28],
128 Circularity [29], Aspect Ratio (Length vs. Width Ratio of leaf) [29], Roundness [29],
129 Solidity [29], Bending Energy [30] and Elliptic Fourier Descriptors (EFD) combined

130 with Principal Component Analysis [31]. All of the methods showed with a statistical
131 significance ($p < 0.05$, Welch's t -test, $n=12$) that tooth protrusions in *epfl2* are smaller
132 than those of wild type (Figure S2I-S2O). Among them, the Solidity method captured the
133 difference in the tooth size most significantly according to F value (variance between
134 genotypes per variance among individuals within the same genotype). Therefore, we
135 adopted the Solidity method to further compare tooth growth levels among *epfl2*,
136 *er*-family and their multiple mutants (Figure 2A), and defined '1-Solidity' as an index of
137 tooth growth level. All the tested mutants showed significant differences in the tooth
138 growth level from the wild type, while no or only small differences were observed among
139 the mutants (Figure 2B). These quantitative analyses support the notion that *EPFL2* and
140 *ER* family genetically act in the same pathway for the tooth growth.

141 To address whether EPFL2 peptide physically interacts with each ER-family
142 receptor, co-immunoprecipitation experiments were performed. FLAG-tagged EPFL2
143 (EPFL2-FLAG) and each of GFP-tagged ER-family receptors without kinase domains
144 (ER Δ K-GFP, ERL1 Δ K-GFP and ERL2 Δ K-GFP) were co-expressed in *Nicotiana*
145 *benthamiana* leaves. When the receptors were immuno-precipitated using anti-GFP
146 antibody, EPFL2-FLAG was detected in the precipitated fractions (Figure 2C), indicating
147 their physical interaction. On the basis of these genetic and biochemical evidence, we
148 conclude that EPFL2 peptide and ER-family receptors constitute ligand-receptor pairs
149 acting for tooth growth.

150

151 ***EPFL2* and *ER* family negatively regulate auxin responses in leaf margin**

152 Auxin responses are restricted to tips of initiating and growing teeth, which is
153 crucial for tooth development [16-19]. To examine relationships between the *EPFL2*
154 activity and the auxin response, the auxin response reporter *DR5::GFP* was analyzed in
155 *epfl2* and *er*-family mutants (Figure 3). In wild type, the *DR5::GFP* expression is
156 restricted to the tip of growing tooth primordia in a later stage of tooth development
157 (Figure 3A). In an early stage, GFP signals were detected also in vascular cells as well as
158 in the tooth tips (Figure 3F). In *epfl2*, *er erl1*, *er erl2* and *erl1 erl2* mutants, *DR5::GFP*
159 signals spread to the surrounding regions of tooth tips in the later stage (Figure 3B-3E).
160 This phenotype was detected even in the early stage of tooth development: the GFP
161 signals are visible in tip periphery regions along the leaf margin (Figure 3G-3J, dashed
162 rectangles; quantification of GFP fluorescence intensity in the rectangles is shown in 3K).
163 In contrast, the overexpression of *EPFL2* by *CaMV 35S* promoter (*35S::EPFL2*; Figure
164 S3A) reduced the *DR5::GFP* expression at growing tooth tips (Figure 3L-3N, dashed
165 circles; 3O, quantification), showing that the *EPFL2* signal represses the auxin response.
166 These observations indicate that *EPFL2* and *ER* family restrict the auxin response to a
167 small number of cells at the tooth tip during the tooth growth. The ectopic *EPFL2*
168 overexpression conferred a reduction in stomatal density (Figure S3B-S3D), which is
169 mediated by the *ER*-family signaling [26]. This further supports the conclusion that
170 *EPFL2* acts through the *ER*-family (Figure 2).

171

172 **The auxin response organizes the expression patterns of *EPFL2* and *ERL2***

173 The expression pattern of *ERL2pro::GUS* at the tooth tip (Figure 1Q) resembles
174 that of *DR5* reporters (Figure 3A, 3F and 4A). By contrast, the *EPFL2pro::GUS* pattern

175 appears to be inversely correlated with those of *ERL2* and *DR5* reporters (Figure 1G, 1Q
176 and 4A). To examine these relationships, the expression patterns were analyzed after
177 auxin polar transport was chemically perturbed by N-1-naphthylphthalamic acid (NPA).
178 In NPA-treated plants, *ERL2pro::GUS* and *DR5::GUS* similarly exhibited broad
179 expression along the leaf margin except for the basal part (Figure S4A and S4B). On the
180 other hand, *EPFL2pro::GUS* expression was restricted to the basal part (Figure S4C),
181 clearly showing inverse correlation with those of *ERL2pro::GUS* and *DR5::GUS*.
182 Collectively, these results suggest that auxin may induce *ERL2*, while it represses *EPFL2*.
183 To address this, exogenous auxin was applied to *ERL2pro::GUS* and *EPFL2pro::GUS*
184 plants. To avoid complications arising from auxin transport, we used a synthetic auxin
185 2,4-Dichlorophenoxyacetic acid (2,4-D), which is not transported by auxin efflux carriers
186 [32]. Upon the 2,4-D application, the *ERL2pro::GUS* expression was enhanced (Figure
187 S4D and S4E), remarkably resembling the *DR5::GUS* pattern (Figure 4A). By contrast,
188 the 2,4-D application diminished the *EPFL2pro::GUS* expression (Figure 4B and 4C).
189 Consistently, the endogenous *ERL2* transcript level increased within a few hours after the
190 2,4-D application (Figure S4F), while the endogenous *EPFL2* transcript level was
191 diminished (Figure 4D). The inhibitory effect of auxin on the *EPFL2* expression is in
192 accordance with the observation that the *EPFL2* expression is eliminated from tooth tips
193 and vascular tissues (Figure 4B), where the auxin response is the highest (Figure 4A). On
194 the basis of these findings, we propose that the auxin response organizes the
195 mutually-exclusive expression patterns of *ERL2* and *EPFL2*.

196

197 **The auxin-responsive patterning of *ER* family and *EPFL2* promotes the tooth**
198 **growth**

199 To examine whether the auxin-responsive expression of *ER*-family is sufficient
200 to promote tooth growth, *ER* was expressed under the *DR5* promoter in *er erl1*. As a
201 result, the *DR5*-driven *ER* expression rescued the toothless phenotype of *er erl1* (Figure
202 4E, 4F, S4G and S4H), demonstrating that the *ER* activity at cells which respond to auxin
203 is sufficient for the tooth growth. We next tested whether the specific expression of
204 *EPFL2* at the peripheral border of growing teeth is sufficient to rescue the tooth growth
205 defects in *epfl2*. For this purpose, *EPFL2* is expressed in *epfl2* mutant under the promoter
206 of *CUP-SHAPED COTYLEDON2 (CUC2)*, which is active at the tooth periphery and
207 repressed by auxin (Figure 4G) [16, 33]. *CUC2pro::EPFL2* rescued the tooth growth
208 defect of *epfl2* (Figure 4H, 4I, S4I and S4J), indicating that the expression of *EPFL2* at
209 the tooth periphery is sufficient to promote the tooth growth. These results highlight the
210 importance of the auxin-responsive patterning of *ER* family and *EPFL2* activities for the
211 tooth growth.

212

213 **Conclusions and model**

214 We have shown that the *EPFL2*-*ER*-family activity represses auxin response. The
215 auxin response in turn represses the *EPFL2* expression and induces the *ERL2* expression.
216 Experimental and computational approaches have been taken to address how auxin
217 response patterns are formed during the tooth initiation step [16-19]. The currently
218 proposed model for the tooth initiation is based on a polar auxin transport to explain the
219 formation of regularly-spaced auxin peaks along leaf margins as well as the formation of

220 a new peak between two existing peaks when the existing peaks are separated apart by
221 tissue growth [16, 34]. In contrast to the tooth initiation process, little has been studied
222 about the molecular basis for the maintenance of a single peak of the auxin response at
223 each tooth tip in the tooth growth step. Our findings establish that the EPFL2-ER-family
224 ligand-receptor pairs restrict the auxin response to the tip of the growing tooth.

225 *CUC2* and its negative regulator *microRNA164* (*miR164*) have been recognized
226 as key regulators of leaf serration [18, 33, 35]. *cuc2-ID*, the *miR164*-resistant dominant
227 allele of *CUC2*, enhances the tooth outgrowth (Figure S4K and S4L) [35]. To address a
228 relationship between *CUC2*/*miR164* and EPFL2-ER-family systems, we constructed
229 *cuc2-ID epfl2* double mutant. *cuc2-ID epfl2* showed obvious teeth even in mature leaves
230 (Figure S4M and S4N), showing that *CUC2* can promote the tooth growth in an
231 *EPFL2*-independent manner. On the other hand, teeth of *cuc2-ID epfl2* were smaller than
232 those of *cuc2-ID* (Figure S4L and S4N), indicating that *EPFL2* is able to act
233 independently of *miR164*. Other transcription factors have been also reported as
234 significant contributors to serration, including BEL1-LIKE HOMEODOMAIN (BLH),
235 KNOTTED1-LIKE HOMEODOMAIN (KNOX), TEOSINTE
236 BRANCHED/CYCLOIDEA/PCF (TCP) and SQUAMOSA PROMOTER-BINDING
237 PROTEIN LIKE (SPL) proteins [36-38]. It would be interesting to investigate how these
238 factors are orchestrated with EPFL2 and CUC2 to determine the extent of leaf serration.

239 We propose a model that explains how EPFL2 and ER family specify leaf margin
240 morphogenesis (Figure 4J). During tooth growth, the auxin response transiently becomes
241 broader due to proliferation of the tip-located cells showing the auxin response and/or *de*
242 *novo* auxin response at their daughter cells (Figure 4J, left to center). The cells

243 responding to auxin cell-autonomously increases the *ER*-family expression (Figure 4J,
244 center). At the same time, since the the *EPFL2* expression is de-repressed in the cells that
245 do not show the auxin response, EPFL2 peptides are produced in the tooth peripheral
246 cells neighboring to the cells responding to auxin at the tooth tip (Figure 4J, center).
247 Secreted EPFL2 peptides are perceived by ER-family proteins in the cells neighboring to
248 the EPFL2-producing cells. This activation of ER-family signaling cell-autonomously
249 suppresses the auxin response (Figure 4J, center to right). This suppression might be
250 mediated by *IAA8/9*, which act redundantly for the leaf tooth growth after initiation like
251 *EPFL2* [39]. These processes continually occur during tooth growth. This circuit enables
252 the highly localized auxin response at the tooth tip and simultaneously keeps the
253 elimination of the *EPFL2* expression from the tip. The feedback regulation between the
254 EPFL2-ER-family system and the auxin response likely represents a novel framework for
255 maintaining auxin responses in growing tissues.

256 The final leaf shape is determined through two distinct processes: the primary
257 morphogenesis that patterns the number and position of primordia of teeth, lobes and
258 leaflets at the initiation step and the secondary morphogenesis that regulates the growth
259 level and direction of developing primordia and surrounding tissues [40]. The impact of
260 the latter process on the leaf shape variation has been shown by the studies using
261 compound-leafed species *Lepidium* [41]. Our findings identify the EPFL2-ER-family
262 system as a regulator of secondary morphogenesis. *EPFL2* belongs to a subclade of
263 *EPFL* family that had not been characterized until this study (Figure 1A), and members
264 of this subclade are well conserved in diverse vascular plants [20]. Further studies on

265 *EPFLs* of this subclade in diverse plant species might provide a novel picture of how the
266 peptide-receptor signaling contributes to a variety of leaf shapes.

267 **Accession numbers**

268 The Arabidopsis Genome Initiative identifiers for the genes referred in this study
269 are as follows: *EPF1* (At2g20875), *EPF2* (At1g34245), *EPFL1* (At5g10310), *EPFL2*
270 (At4g37810), *EPFL3* (AT3G13898), *EPFL4/CLL2* (At4g14723), *EPFL5/CLL1*
271 (At3g22820), *EPFL6/CHAL* (At2g30370), *EPFL7* (AT1G71866), *EPFL8* (AT1G80133),
272 *EPFL9/STOMAGEN* (At4g12970), *ER* (At2g26330), *ERL1* (At5g62230), *ERL2*
273 (At5g07180), *CUC2* (At5g53950).

274

275 **Supplemental Information**

276 Supplemental Information includes Supplemental Experimental Procedures, four
277 figures and two tables.

278 **Author contributions**

279 T.T., M.T., K.U.T. and N.U. designed research; T.T., S.O., J.S.L. and N.U.
280 performed research; T.T., S.O., J.S.L. M.A., M.T., K.U.T. and N.U. analyzed and
281 discussed data; T.T., K.U.T. and N.U. wrote the paper

282

283 **Acknowledgments**

284 We thank Tatsuo Kakimoto (Osaka Univ.) and Tom J. Guilfoyle (Univ. of
285 Missouri) for providing *EPFL2pro::GUS* plasmid and *DR5::GUS* seeds, respectively. We
286 also acknowledge Shuka Ikematsu (WPI-ITbM) for outcrossing *epfl2*, and Yoshikatsu
287 Sato (WPI-ITbM Live Imaging Center) for generous support in confocal microscopy. The
288 microscopic work was partly supported by Japan Advanced Plant Science Network. This
289 work was supported by MEXT/JSPS KAKENHI (Grant numbers JP26113507,
290 JP26291057 and JP16H01237 to K.U.T; Grant numbers JP25114511, JP26113707 and
291 JP16H01462 to N.U.), and Toyoaki foundation (to N.U.) and Gordon and Betty Moore
292 Foundation (GBMF3035 to K.U.T). K.U.T. is an HHMI-GBMF Investigator.

293

294 **Reference**

295

- 296 1. Tavormina, P., De Coninck, B., Nikonorova, N., De Smet, I., and Cammue, B.P.A.
297 (2015). The Plant Peptidome: An Expanding Repertoire of Structural Features and
298 Biological Functions. *Plant Cell* 27, 2095-2118.
- 299 2. Tameshige, T., Hirakawa, Y., Torii, K.U., and Uchida, N. (2015). Cell walls as a
300 stage for intercellular communication regulating shoot meristem development.
301 *Frontiers in Plant Science* 6, e324.
- 302 3. Richardson, L.G.L., and Torii, K.U. (2013). Take a deep breath: peptide signalling
303 in stomatal patterning and differentiation. *Journal of Experimental Botany* 64,
304 5243-5251.
- 305 4. Hara, K., Kajita, R., Torii, K.U., Bergmann, D.C., and Kakimoto, T. (2007). The
306 secretory peptide gene EPF1 enforces the stomatal one-cell-spacing rule. *Genes &*
307 *Development* 21, 1720-1725.
- 308 5. Hara, K., Yokoo, T., Kajita, R., Onishi, T., Yahata, S., Peterson, K.M., Torii, K.U.,
309 and Kakimoto, T. (2009). Epidermal Cell Density is Autoregulated via a Secretory
310 Peptide, EPIDERMAL PATTERNING FACTOR 2 in Arabidopsis Leaves. *Plant*
311 *and Cell Physiology* 50, 1019-1031.
- 312 6. Hunt, L., and Gray, J.E. (2009). The Signaling Peptide EPF2 Controls
313 Asymmetric Cell Divisions during Stomatal Development. *Current Biology* 19,
314 864-869.
- 315 7. Hunt, L., Bailey, K.J., and Gray, J.E. (2010). The signalling peptide EPFL9 is a
316 positive regulator of stomatal development. *New Phytologist* 186, 609-614.

- 317 8. Sugano, S.S., Shimada, T., Imai, Y., Okawa, K., Tamai, A., Mori, M., and
318 Hara-Nishimura, I. (2010). Stomagen positively regulates stomatal density in
319 Arabidopsis. *Nature* 463, 241-U130.
- 320 9. Kondo, T., Kajita, R., Miyazaki, A., Hokoyama, M., Nakamura-Miura, T., Mizuno,
321 S., Masuda, Y., Irie, K., Tanaka, Y., Takada, S., et al. (2010). Stomatal Density is
322 Controlled by a Mesophyll-Derived Signaling Molecule. *Plant and Cell*
323 *Physiology* 51, 1-8.
- 324 10. Lee, J.S., Kuroha, T., Hnilova, M., Khatayevich, D., Kanaoka, M.M., McAbee,
325 J.M., Sarikaya, M., Tamerler, C., and Torii, K.U. (2012). Direct interaction of
326 ligand-receptor pairs specifying stomatal patterning. *Genes & Development* 26,
327 126-136.
- 328 11. Lee, J.S., Hnilova, M., Maes, M., Lin, Y.-C.L., Putarjunan, A., Han, S.-K., Avila,
329 J., and Torii, K.U. (2015). Competitive binding of antagonistic peptides fine-tunes
330 stomatal patterning. *Nature* 522, 439-443.
- 331 12. Niwa, T., Kondo, T., Nishizawa, M., Kajita, R., Kakimoto, T., and Ishiguro, S.
332 (2013). EPIDERMAL PATTERNING FACTOR LIKE5 Peptide Represses
333 Stomatal Development by Inhibiting Meristemoid Maintenance in *Arabidopsis*
334 *thaliana*. *Bioscience Biotechnology and Biochemistry* 77, 1287-1295.
- 335 13. Abrash, E.B., Davies, K.A., and Bergmann, D.C. (2011). Generation of Signaling
336 Specificity in *Arabidopsis* by Spatially Restricted Buffering of Ligand-Receptor
337 Interactions. *Plant Cell* 23, 2864-2879.
- 338 14. Uchida, N., Lee, J.S., Horst, R.J., Lai, H.H., Kajita, R., Kakimoto, T., Tasaka, M.,
339 and Torii, K.U. (2012). Regulation of inflorescence architecture by intertissue

- 340 layer ligand-receptor communication between endodermis and phloem.
341 Proceedings of the National Academy of Sciences of the United States of America
342 *109*, 6337-6342.
- 343 15. Uchida, N., and Tasaka, M. (2013). Regulation of plant vascular stem cells by
344 endodermis-derived EPFL-family peptide hormones and phloem-expressed
345 ERECTA-family receptor kinases. *Journal of Experimental Botany* *64*,
346 5335-5343.
- 347 16. Bilsborough, G.D., Runions, A., Barkoulas, M., Jenkins, H.W., Hasson, A.,
348 Galinha, C., Laufs, P., Hay, A., Prusinkiewicz, P., and Tsiantis, M. (2011). Model
349 for the regulation of *Arabidopsis thaliana* leaf margin development. Proceedings
350 of the National Academy of Sciences of the United States of America *108*,
351 3424-3429.
- 352 17. Hay, A., Barkoulas, M., and Tsiantis, M. (2006). ASYMMETRIC LEAVES1 and
353 auxin activities converge to repress BREVIPEDICELLUS expression and
354 promote leaf development in *Arabidopsis*. *Development* *133*, 3955-3961.
- 355 18. Kawamura, E., Horiguchi, G., and Tsukaya, H. (2010). Mechanisms of leaf tooth
356 formation in *Arabidopsis*. *Plant Journal* *62*, 429-441.
- 357 19. Kasprzewska, A., Carter, R., Swarup, R., Bennett, M., Monk, N., Hobbs, J.K., and
358 Fleming, A. (2015). Auxin influx importers modulate serration along the leaf
359 margin. *Plant Journal* *83*, 705-718.
- 360 20. Takata, N., Yokota, K., Ohki, S., Mori, M., Taniguchi, T., and Kurita, M. (2013).
361 Evolutionary Relationship and Structural Characterization of the EPF/EPFL Gene
362 Family. *Plos One* *8*, 6.

- 363 21. Torii, K.U., Mitsukawa, N., Oosumi, T., Matsuura, Y., Yokoyama, R., Whittier,
364 R.F., and Komeda, Y. (1996). The arabidopsis ERECTA gene encodes a putative
365 receptor protein kinase with extracellular leucine-rich repeats. *Plant Cell* 8,
366 735-746.
- 367 22. Malinowski, R., Kasprzewska, A., and Fleming, A.J. (2011). Targeted
368 manipulation of leaf form via local growth repression. *Plant Journal* 66, 941-952.
- 369 23. Shpak, E.D., Berthiaume, C.T., Hill, E.J., and Torii, K.U. (2004). Synergistic
370 interaction of three ERECTA-family receptor-like kinases controls Arabidopsis
371 organ growth and flower development by promoting cell proliferation.
372 *Development* 131, 1491-1501.
- 373 24. Bowman, J. (1994). *Arabidopsis: An Atlas of Morphology and Development*, 1
374 Edition, (New York: Springer-Verlag).
- 375 25. Chen, M.K., Wilson, R.L., Palme, K., Ditengou, F.A., and Shpak, E.D. (2013).
376 ERECTA Family Genes Regulate Auxin Transport in the Shoot Apical Meristem
377 and Forming Leaf Primordia. *Plant Physiology* 162, 1978-1991.
- 378 26. Shpak, E.D., McAbee, J.M., Pillitteri, L.J., and Torii, K.U. (2005). Stomatal
379 patterning and differentiation by synergistic interactions of receptor kinases.
380 *Science* 309, 290-293.
- 381 27. Uchida, N., Shimada, M., and Tasaka, M. (2013). ERECTA-Family Receptor
382 Kinases Regulate Stem Cell Homeostasis via Buffering its Cytokinin
383 Responsiveness in the Shoot Apical Meristem. *Plant and Cell Physiology* 54,
384 343-351.
- 385 28. Hasson, A., Plessis, A., Blein, T., Adroher, B., Grigg, S., Tsiantis, M., Boudaoud,

- 386 A., Damerval, C., and Laufs, P. (2011). Evolution and Diverse Roles of the
387 CUP-SHAPED COTYLEDON Genes in Arabidopsis Leaf Development. *Plant*
388 *Cell* 23, 54-68.
- 389 29. Chitwood, D.H., Ranjan, A., Kumar, R., Ichihashi, Y., Zumstein, K., Headland,
390 L.R., Ostria-Gallardo, E., Aguilar-Martinez, J.A., Bush, S., Carriedo, L., et al.
391 (2014). Resolving Distinct Genetic Regulators of Tomato Leaf Shape within a
392 Heteroblastic and Ontogenetic Context. *Plant Cell* 26, 3616-3629.
- 393 30. Backhaus, A., Kuwabara, A., Bauch, M., Monk, N., Sanguinetti, G., and Fleming,
394 A. (2010). leafprocessor: a new leaf phenotyping tool using contour bending
395 energy and shape cluster analysis. *New Phytologist* 187, 251-261.
- 396 31. Chitwood, D.H., Headland, L.R., Kumar, R., Peng, J., Maloof, J.N., and Sinha,
397 N.R. (2012). The Developmental Trajectory of Leaflet Morphology in Wild
398 Tomato Species. *Plant Physiology* 158, 1230-1240.
- 399 32. Delbarre, A., Muller, P., Imhoff, V., and Guern, J. (1996). Comparison of
400 mechanisms controlling uptake and accumulation of 2,4-dichlorophenoxy acetic
401 acid, naphthalene-1-acetic acid, and indole-3-acetic acid in suspension-cultured
402 tobacco cells. *Planta* 198, 532-541.
- 403 33. Nikovics, K., Blein, T., Peaucelle, A., Ishida, T., Morin, H., Aida, M., and Laufs, P.
404 (2006). The balance between the MIR164A and CUC2 genes controls leaf margin
405 serration in Arabidopsis. *Plant Cell* 18, 2929-2945.
- 406 34. Nakamasu, A., Nakayama, H., Nakayama, N., Suematsu, N.J., and Kimura, S.
407 (2014). A Developmental Model for Branching Morphogenesis of Lake Cress
408 Compound Leaf. *Plos One* 9, 7.

- 409 35. Larue, C.T., Wen, J.Q., and Walker, J.C. (2009). A microRNA-transcription factor
410 module regulates lateral organ size and patterning in Arabidopsis. *Plant Journal* 58,
411 450-463.
- 412 36. Kumar, R., Kushalappa, K., Godt, D., Pidkowich, M.S., Pastorelli, S., Hepworth,
413 S.R., and Haughn, G.W. (2007). The Arabidopsis BEL1-LIKE HOMEODOMAIN
414 proteins SAW1 and SAW2 act redundantly to regulate KNOX expression spatially
415 in leaf margins. *Plant Cell* 19, 2719-2735.
- 416 37. Kimura, S., Koenig, D., Kang, J., Yoong, F.Y., and Sinha, N. (2008). Natural
417 variation in leaf morphology results from mutation of a novel KNOX gene.
418 *Current Biology* 18, 672-677.
- 419 38. Rubio-Somoza, I., Zhou, C.M., Confraria, A., Martinho, C., von Born, P.,
420 Baena-Gonzalez, E., Wang, J.W., and Weigel, D. (2014). Temporal Control of
421 Leaf Complexity by miRNA-Regulated Licensing of Protein Complexes. *Current*
422 *Biology* 24, 2714-2719.
- 423 39. Koenig, D., Bayer, E., Kang, J., Kuhlemeier, C., and Sinha, N. (2009). Auxin
424 patterns *Solanum lycopersicum* leaf morphogenesis. *Development* 136,
425 2997-3006.
- 426 40. Champagne, C., and Sinha, N. (2004). Compound leaves: equal to the sum of their
427 parts? *Development* 131, 4401-4412.
- 428 41. Bharathan, G., Goliber, T.E., Moore, C., Kessler, S., Pham, T., and Sinha, N.R.
429 (2002). Homologies in leaf form inferred from KNOXI gene expression during
430 development. *Science* 296, 1858-1860.
- 431

432 **Figure Legends**

433

434 Figure 1. *EPFL2* and *ER* family are required for leaf tooth growth.

435 (A) Neighbor-joining unrooted phylogenetic tree of EPFL members. *EPFL2* is
436 highlighted in green. The previously characterized members are indicated by cyan and
437 orange underlines. Scale bar: 0.1 amino acid substitutions per site.

438 (B, D, H, J and L) Mature seventh leaves of wild type (abbreviated as WT in all figures)
439 (B), *epfl2* (D), *er erl1* (H), *er erl2* (J) and *erl1 erl2* (L). Right panels are magnified views
440 of leaf edges. Curled leaf was flattened with incisions indicated by broken lines.

441 (C, E, I, K and M) wild-type (C), *epfl2* (E), *er erl1* (I), *er erl2* (K) and *erl1 erl2* (M)
442 young ninth leaves of 1 mm in length.

443 (F and N) Superimposition of leaf outlines from *epfl2* (F) and *erl1 erl2* (N) with those
444 from wild type. X- and Y-values of each leaf are scaled proportionally so that each leaf
445 size is one and thus the size of half leaves shown in panels is 0.5. The original leaf sizes
446 of *epfl2*, *erl1 erl2* and wild type are $2.82 \pm 0.47 \text{ mm}^2$ (mean \pm SEM, n = 10), 2.30 ± 0.39
447 mm^2 (n = 10) and $2.70 \pm 0.29 \text{ mm}^2$ (n = 12), respectively. The same wild type data are
448 shown in both panels. The outlines are shown as line plot (left). The positions of each
449 tooth tip (top right) and sinus (bottom right) are shown as scatter plots.

450 (G, O-Q) GUS patterns of *EPFL2pro::GUS* (G), *ERpro::GUS* (O), *ERL1pro::GUS* (P)
451 and *ERL2pro::GUS* (Q) in young sixth leaf of 1 mm in length. The right panels are
452 magnified views.

453 Arrowheads: teeth. Scale bars: B, D, H, J and L, 1 mm; C, E, G, I, K, M and O-Q 100
454 μm .

455

456 Figure 2. Genetic and physical interaction between EPFL2 and ER-family.

457 (A) Black-and-white images of young leaves from multiple mutants of *EPFL2* and *ER*
458 family as well as their parental lines.

459 (B) Tooth growth levels of young leaves from multiple mutants of *EPFL2* and *ER* family
460 and their parental lines. Mean values and the standard errors are shown. n = 12, 12, 13,
461 10, 15, 14, 14, and 12 for wild type, *epfl2*, *erl1 erl2*, *erl1 erl2 epfl2*, *er erl1*, *er erl1 epfl2*,
462 *er erl2* and *er erl2 epfl2*, respectively. Letters indicate significant differences ($p < 0.05$)
463 determined by Tukey's HSD test. See main text and Supplemental Experimental
464 Procedures for the calculation method.

465 (C) Co-immunoprecipitation assays of FLAG-tagged EPFL2 and GFP-tagged
466 kinase-truncated ER-family proteins. The immuno-precipitated (IP) fractions by anti-GFP
467 antibody were separated by SDS-PAGE, and the precipitated proteins were detected by
468 anti-GFP and anti-FLAG antibodies.

469

470 Figure 3. *EPFL2* and *ER* family restrict the auxin response to the tooth tip.

471 (A-J and L-N) Z-projected confocal micrographs of growing teeth in wild type (A, F and
472 L), *epfl2* (B and G), *er erl1* (C and H), *er erl2* (D and I) *erl1 erl2* (E and J) and
473 *35S::EPFL2* (M and N). Auxin responses are indicated by *DR5::GFP* (green and color
474 look-up-tables to the right of I and M). Note that detector settings for GFP fluorescence
475 are different among three groups ('A-E', 'F-J' and 'L-N') according to each dynamic
476 range. The leaf shape is shown by chlorophyll fluorescence (magenta) in A-E or
477 transmitted-light images (gray scale) in F-J and L-N. Growing leaves at the later stage

478 (A-E; sixth or seventh leaves of 14-day-old plants) and the early stage (F-J and L-N;
479 seventh leaves of 13-day-old plants) are used for analysis. Dashed rectangles (F-J) and
480 circles (L-N) indicate the tooth periphery regions and tip regions used to measure the
481 GFP intensity in K and O, respectively. Scale bars: 100 μm
482 (K and O) Bar plots of GFP fluorescence intensity. Mean values per pixel and the
483 standard errors from the indicated regions in F-J (K) and in L-N (O) are shown for each
484 line. $n = 10, 13, 15, 16$ and 17 for wild type, *epfl2*, *er erl1*, *er erl2* and *erl1 erl2*,
485 respectively (K). $n = 9, 5$ and 10 for wild type, *35::EPFL2* line #1 and #2, respectively
486 (O). Asterisks indicate significant differences ($p < 0.05$ in Welch's *t*-test) from the
487 wild-type data.

488

489 Figure 4. The auxin-responsive patterning of the *EPFL2* and *ER*-family expression
490 promotes the tooth growth.

491 (A) *DR5::GUS* pattern in a young leaf.

492 (B and C) *EPFL2pro::GUS* patterns in mock- (A) and 2,4-D-treated (B) young leaves.

493 (D) Expression levels of *EPFL2* after 2,4-D treatment measured by real-time RT-PCR.

494 The expression levels were normalized with respect to that of *ACTIN2*. The normalized
495 value at 0 hour was set to 1. Thirty shoot apices were collected as a pool for each sample
496 ($n = 4$). Asterisks indicate significant differences ($p < 0.05$ in Welch's *t*-test) from the
497 0-hour data. Error bars: standard error of the mean.

498 (E, F, H and I) Mature leaf edges of *er erl1* (E), *er erl1 DR5::ER* (F), *epfl2* (H) and *epfl2*
499 *CUC2pro::EPFL2* (I). See also Figure S4G-S4J for other independent transformant lines.

500 (G) *CUC2pro::GUS* pattern in a young leaf.

501 Arrowheads: teeth. Scale bars: A-C and G, 100 μm ; E, F, H and I, 1 mm.
502 (J) A model for the maintenance of the auxin response at the growing tooth tip mediated
503 by the feedback regulation between the EPFL2-ER-family system and the auxin response.
504 See the detailed explanation in main text. Cells responding to auxin, green; EPFL2
505 peptides, blue dots; ER-family receptors, red.

Figure 1

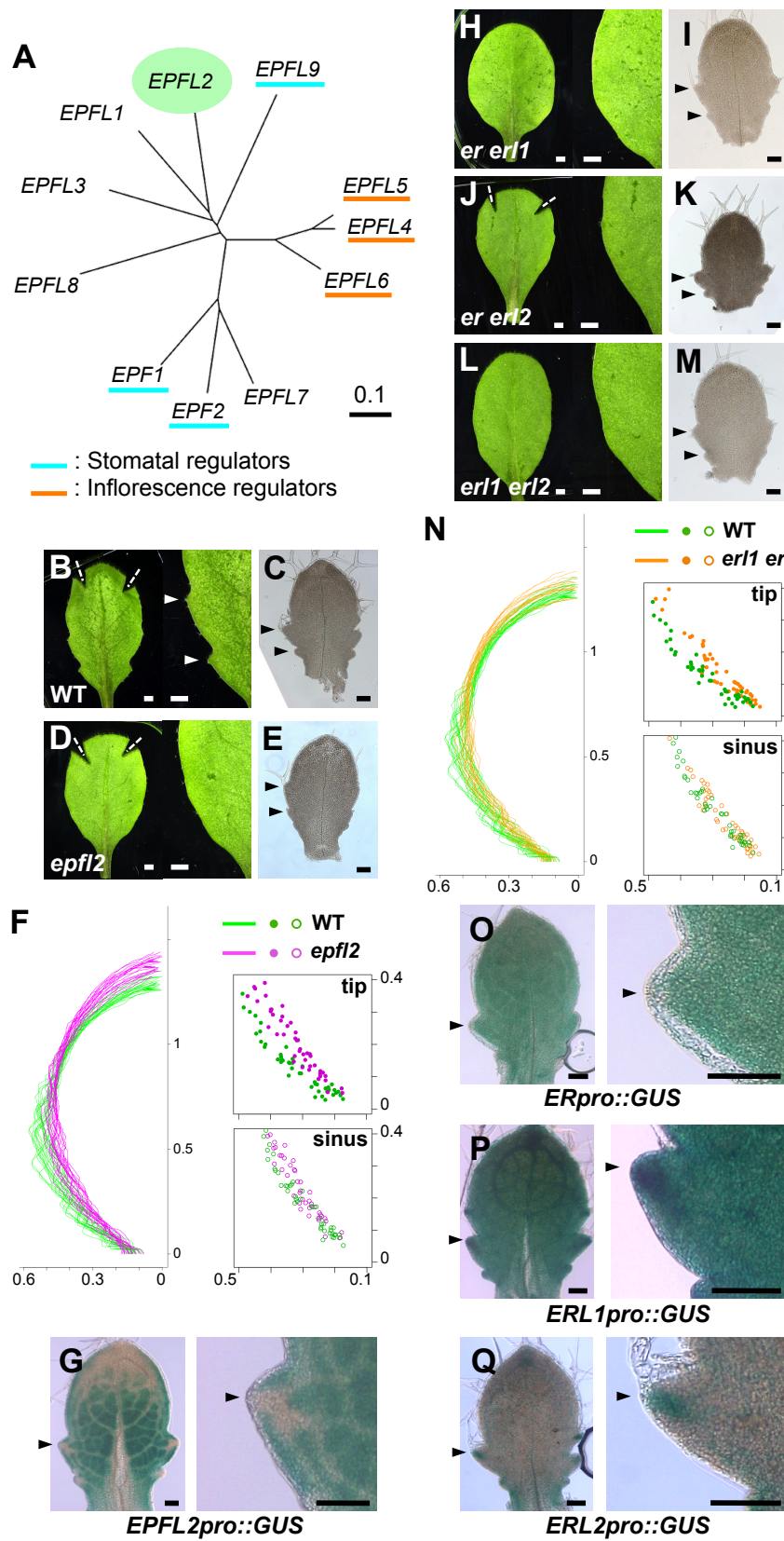


Figure 2

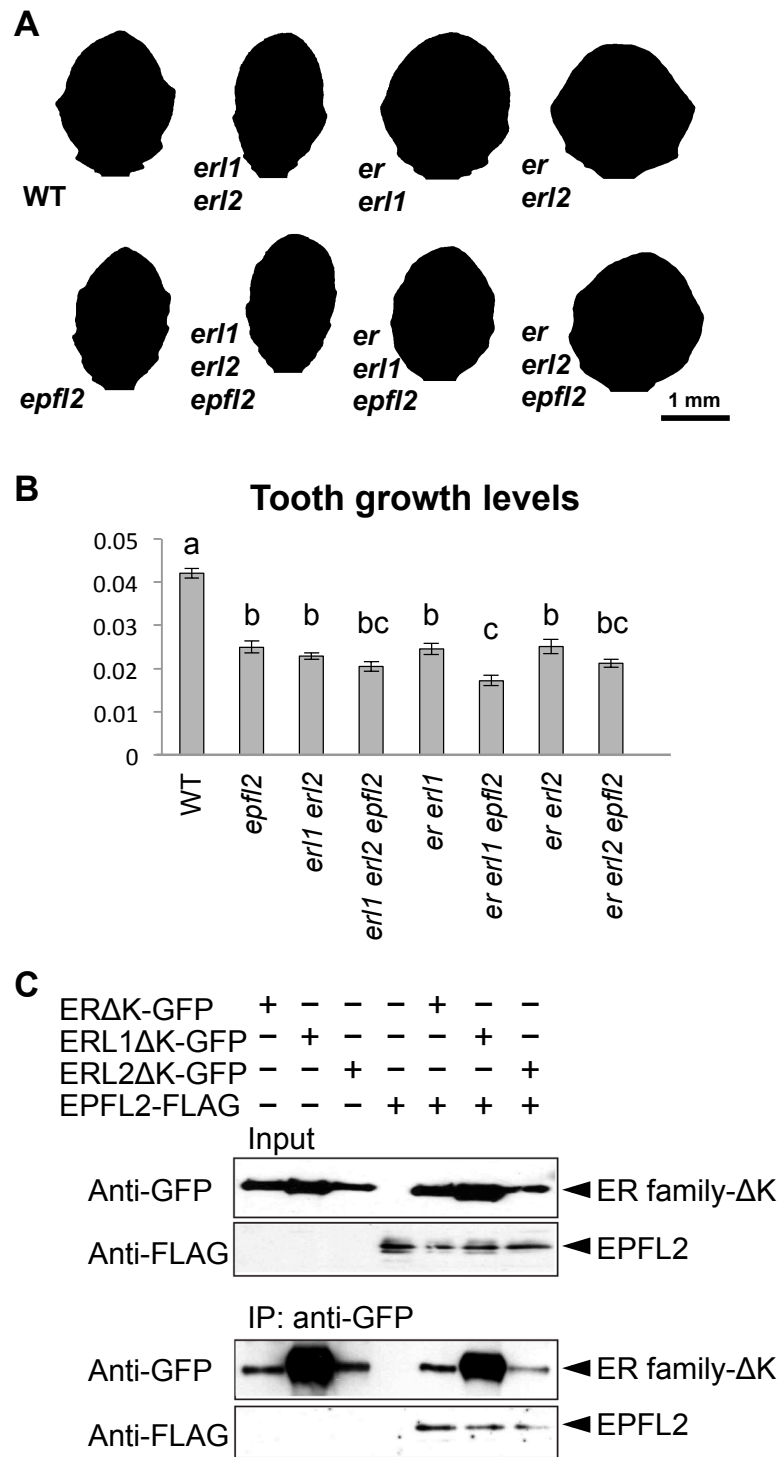


Figure 3

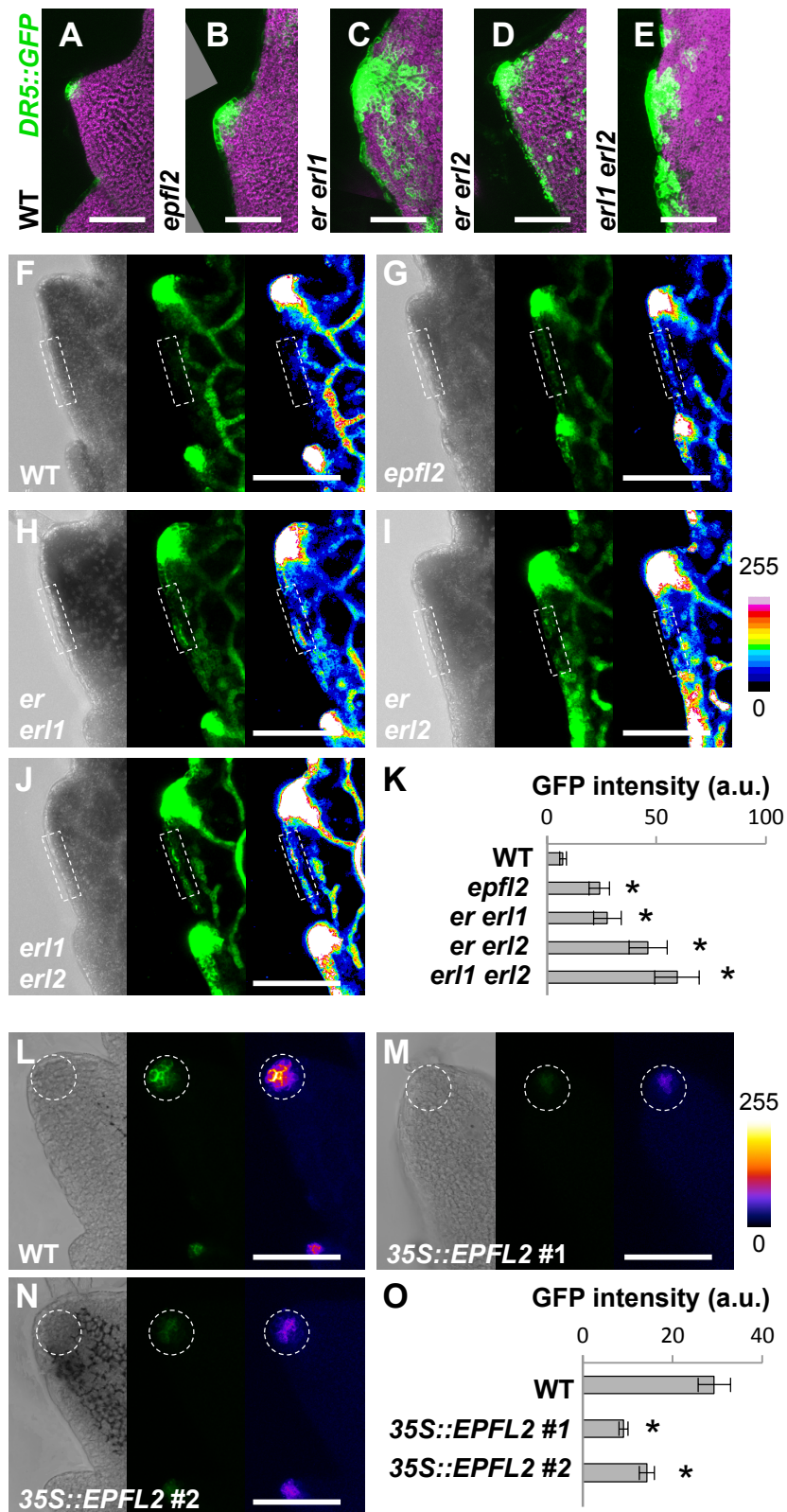


Figure 4

